CHEMICAL ENGINEERING TRANSACTIONS Volume 17, 2009
Editor Sauro Pierucci

 ISBN 978-88-95608-01-3 ISSN 1974-9791
DOI: 10.3303/CET0917208

Results of Modelling of Coupled Endo and Exothermic Reactions in a Catalytic Microstructured Reactor

P. Ciambelli, L. Malangone, S. Vaccaro
Department of Chemical and Food Engineering, University of Salerno
Via ponte don Melillo 84084 – Fisciano (SA) Italy

The computational flow modeling (CFD) may be a successful method to predict and/or design new reactors or chemical systems. With the development of high performance computers and advances in numerical techniques and algorithms new challenges in prediction of system performances may be considered and the classic limitations, which imposed drastic simplifications of the real system geometry, may be overcome.
In this study the mathematical modeling of a real catalytic microstructured plate reactor for the production of hydrogen was performed in 3D geometry. The reactor pertains to the recently developed heat exchanger reactors in which reaction systems use directly heat from an exothermic reaction (for instance combustion) to sustain endothermic reforming reactions. Experimental performance of the reactor is presented in another paper of this Conference (Ciambelli et al., 2009) while here the description of such a performance through the model results and the limits of the modeling are discussed. The catalytic contribution of both reactions was modeled considering the classic Langmuir-Hinshelwood surface kinetic theory.
The advantage of using a real 3D geometry configuration was due to the possibility of considering the importance of the boundary effects that cannot be properly taken into account when 2D modelling is employed. This is particularly true when significant heat loss through the boundaries verify. The model neglects radiant heat transfer, while convective and conductive heat dispersions were evaluated imposing external wall temperature profiles deduced from experimental tests: these experiments were performed in order to validate the model using methane as combustion and reforming fuel.
The feasibility of the model proposed may show its potential in fast and easy implementation of several combustion and reforming processes so to significantly enhance the performance prediction of real processes.

1. Reactor Scheme

A 3D scheme of the modeled reactor is shown in Figure 1 where the main parts are indicated. Given the symmetries with respect to the x-y plane and the x-z plane, only one fourth of the complete reactor is sketched. This represents also the actual modelled portion of the reactor whose operating performance has been simulated. The reactor is made of three channels with a parallelepiped shape: the central one, where reforming

Please cite this article as: Ciambelli P., Malangone L. and Vaccaro S., (2009), Results of modelling of coupled endo and exothermic reactions in a catalytic microstructured reactor, Chemical Engineering Transactions, 17, 1245-1250 DOI: 10.3303/CET0917208

gases are fed, is 50 mm long, 10 mm wide and 3.0 mm thick while the lateral channels for combustion gases are each 50 mm long, 10 mm wide, 1.5 mm thick. However, the channels have two protruding rounded edges, which actually makes the total channels length 60 mm, and are separated each other by metallic foils (0.5 mm tick) onto which different catalysts were deposited on the opposite faces (Figure 1). The reactants flow patterns are also shown in Figure 1. Both the reforming and the combustion streams

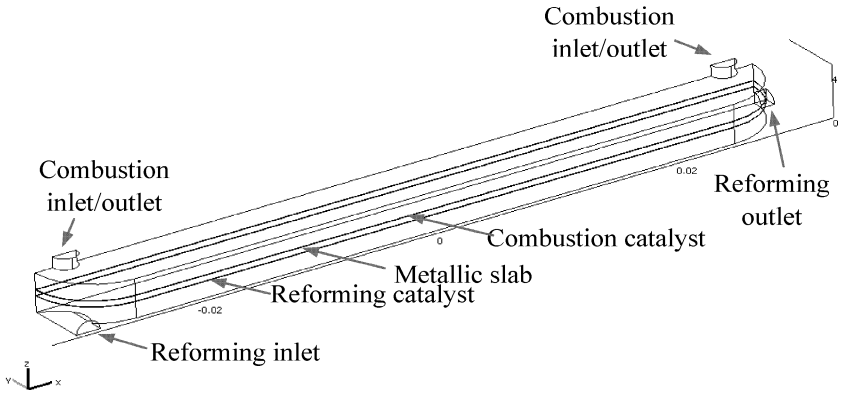

enters the reactor along a direction perpendicular to the channel axis (x direction) although the reforming one moves along y and that of combustion along z. The flow in the combustion channel can be reversed and, then, the reactor may operate with concurrent (CNC) or countercurrent (CTC) flow patterns of the reactants.

Fig.1: 3D reactor scheme

2. Model

2.1 Model description

A three-dimensional heterogeneous steady-state model has been recently developed by the authors (Vaccaro and Ciambelli, 2008a) in order to describe velocity, concentration and temperature distributions inside the catalytic slabs reactor. The model consists of the material, energy and momentum balances equations for the system in the object and contains the constitutive equations for physical chemistry properties of the reactants species and the kinetic expressions for the reactions as found from the literature. In particular, the rate equations of the methane reforming reaction and the water gas shift reaction are those derived by Xu and Froment (1989), i.e. for a catalyst containing 15.2% Ni supported on MgO-αAl_2O_3. Instead, for the methane total combustion, a rate equation depending linearly on the methane concentration only, as suggested in the literature (Zanfir and Gavriilidis, 2003), and valid for a catalyst containing Pt supported on α-Al_2O_3 has been used. The model, of which a detailed description can be found elsewhere (Vaccaro and Ciambelli 2008a, Vaccaro and Ciambelli, 2008b), assumes that: a) density variations due to change of gas composition and temperature are small so that incompressible Navier-Stokes motion equation applies; b) on the combustion side only the methane total oxidation reaction to H_2O and CO_2 occurs; c) on the reforming side only the methane steam reforming and the water gas shift reactions occurs; d) reactions occur only inside the catalyst layers where, instead, convective momentum is not

present; e) conductive heat transfer is the only transport phenomenon occurring inside the metallic plates; f) as suggested in the literature (Hou and Hughes, 2001), carbon formation and deposition due to side reactions can be neglected by using an excess of steam, that is a steam/methane molar ratio above 1.7; g) body forces are neglected.
According to Figure 1, for each catalyst layer and channel and for the metal foils the due momentum, energy and mass balances were set together with the proper boundary conditions in Cartesian coordinates (x–y–z) (indicated in Figure 1) with dependent variables: velocity components, pressure, temperature (T) and species concentrations (c_i).

2.2 Numerical parameters and case simulation

The finite element solution algorithm was completed using COMSOL Multiphysics (Comsol, Inc., version 3.5). Multiphysics modules of incompressible Navier-Stokes, convection–diffusion and conduction–convection were applied, when appropriate, to the three-phase domains. Predefined mesh sizes, extra coarse with 28056 elements and 274675 number of degree of freedom, were employed.
The simulation was carried out for a given reactor operating condition, for which experimental results were available, that is: reforming channel, total molar feed of 1.367 mol/h with an H_2O/CH_4 ratio of 2.78; combustion channel, total molar feed of 2.441 mol/h with a CH_4/O_2 ratio of 1/1.68. The latter data indicates that the reactant mixtures fed in the combustion channel contain 19 % excess methane with respect to stoichiometric. Such a conditions was chosen because the experiments (Ciambelli et al., 2009) showed that there is a sort of inhibition of methane oxidation when working with stoichiometric or excess air in agreement with findings from literature (Lee et Trimm, 1995). As a consequence, the dependence of feeding oxygen on the kinetics when using a power-law rate expression may be neglected according to literature (Otto, K. 1989; Niwa et al., 1983; Cullis et al.,1983; Kolaczkowski et al.,1996; Garetto et al., 2000). Under the specified feed conditions the mean residence times (τ_{co} and τ_{sr}), in both the reforming and the combustion channels, calculated as ratios between the channel volume and the gas flow rate at the average channel temperature, were 57 ms and 35 ms, respectively.

2.3 Evaluation of reactor performance

The velocity variation in the reactor takes into account the influence of temperature and composition changes so that the global mass balance is satisfied everywhere along the reactor. Reactor performance were evaluated through the methane conversions in the combustion ($X_{ch4\text{-}co}$) and in the reforming ($X_{ch4\text{-}sr}$) channel, calculated by integrating the local molar flow rates over the transverse surface area and by the CO/CO_2 ratio and the H_2 molar concentration (y_{H2}) at the exit of the reforming channel.
As mentioned above, the general expression of the rate equations for the reforming and combustion reactions were those suggested in the literature and employed in previous work by the authors (Vaccaro and Ciambelli, 2008a and b). However, in the present case changes were made in the kinetic parameters (frequency factor and/or apparent activation energy) to match the model results with the experimental findings. In particular, for the combustion rate equation the frequency factor was changed from 4 10^8 s^{-1} to 1.5 10^7 s^{-1} and the activation energy from 90 10^6 to 70 10^6 kJ/mol. Instead, for

the steam reforming rate equation and the water gas shift reaction only the frequency factors were modified by a factor 0.042 and 0.13, respectively.
A further tool used to match the experiments with the model results is the external wall temperature or the boundary conditions. In particular, it has been assumed that the internal surface temperature of the external walls along x and z directions reflects the temperature profiles on the axes of the channels measured in the experiments.
It worth to note that to actually describe the experimental findings of the reactor by the model it is necessary to use the 3D model. This because the external walls through which heat can be transferred inside from an external source or viceversa extends both along a plane parallel to the x-y plane and a plane parallel to the x-z plane and the extension of such walls are comparable. As a results a 2D simulation would have neglect the heat transfer in y direction leading to wrong results.

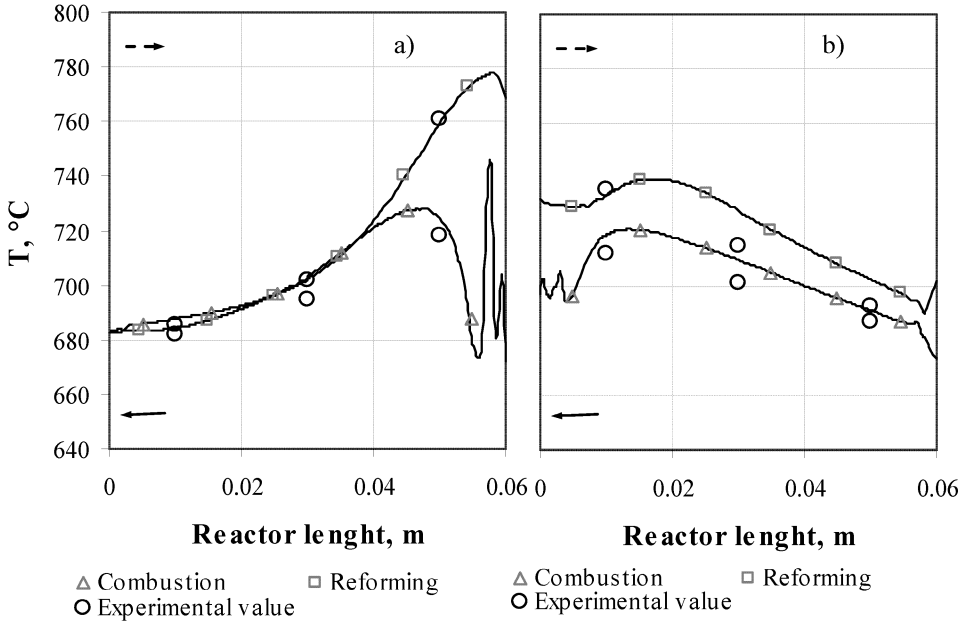

Figure 2 Comparison between calculated temperature profiles on the axes of the reforming and of the combustion channel and temperature measured at three locations along the same axes. Flow pattern: a) CNC. b) CTC . Dashed arrow: reforming flow direction. Solid arrow: combustion flow

3. Results and discussion

3.1 Temperature profiles

Typical calculated temperature axial profiles on the centerlines of the reforming and the combustion channels for the cases of CNC and CTC flow patterns, are reported in Figure 2 a) and b), respectively. Both show that under the tested operating conditions the temperatures inside the reforming channel were almost always higher than those detected in the combustion channels. This effect has been related to the thermal

dissipation through the external walls of the reactor (representing also one of the boundary of the combustion channel) since the heat flux across such walls induced a steep thermal gradient in the combustion channels.
Figure 2 a) and b) also show the comparison between the calculated temperature longitudinal profiles and the measured temperatures along the axes of the reforming and of the combustion channels at three distances from the reactor entrance (0.01, 0.03 and 0.05 m), for the cases of CNC and CTC flow pattern, respectively. It is worth noting that the kinetic parameters employed to obtain such match were the same in both CNC and CTC configurations. Figures 2 a) and b) make evident that in both cases of CNC and CTC the agreement between the measured and calculated temperatures is very good. In particular, the agreement is excellent for the CTC case while reforming channel temperature are overestimated in the case of CNC.

3.2 Methane conversion
Quantitative differences in reactor performance between CNC and CTC flow patterns are shown in Table 1 where the various parameters, defined in section 2.3, are reported. In the same Table the comparison between calculated and measured values of such parameters are also shown. The experimental values indicates a slight prevalence of the performance of the CNC with respect to CTC flow configuration. Indeed, the former configuration gives higher methane conversion, a consequent larger hydrogen production and a lower CO/CO_2 ratio in the reforming channel. Simulation results, however, confirmed the CO/CO_2 ratios but not the values of $X_{CH4\text{-}sr}$ and y_{H2} since both result higher for the CTC case than for the CNC one. Nonetheless, the whole results show that the use of countercurrent and concurrent flow patterns of reactants does not influence significantly the reactor performance. This finding, already found in a previous modelling work (Vaccaro et al. 2008a) in the case of an adiabatic reactor, has been confirmed by the model also under non adiabatic conditions and also verified by the experiments.
The comparison between model results and experimental findings appeared, generally, very good. However, it is worth noting that such an agreement was achieved by appropriately tuning the values of the kinetic parameters pertaining to steam reforming, water gas shift and combustion reactions, and by choosing external walls temperature profiles through trial and error procedures. Nonetheless, it is remarkable that the kinetic parameters fixed with the CNC flow pattern worked also for the CTC one yielding results that well agree with the experiments.

Table 1. Comparison between experimental and calculated reactor performance for both the CNC and CTC reactant flow patterns.

Mode	Flow pattern	$X_{CH4\text{-}co}$, %	$X_{CH4\text{-}sr}$, (%)	$y_{H2,}$ %	CO/CO_2
experimental	CNC	83.40	59.64	64.12	1.57
calculated	CNC	84.77	57.14	62.69	1.85
experimental	CTC	85.40	57.00	62.65	2.55
calculated	CTC	85.18	62.00	64.67	2.49

In any case, the need to choose the reactor external walls temperature profiles represents a limit of the work and of the model. It also suggests that in general the possibility to successfully model a system depends on the possibility to set suitable boundary conditions that may be obtained experimentally. In the case in the object this could be achieved by controlling the reactor external temperature for instance through insertion in a temperature-controlled oven or by immersion in a fused salts bath.

Acknowledgments
The authors gratefully acknowledge the financial support of MIUR under grant PRIN n°2006094333004

4. References

Ciambelli P., Malangone L., Manna M. A., Vaccaro S., 2009, *Experimental Investigation of Endo and Exothermic Reactions Coupling in a Catalytic Microstructured Reactor*. ICheaP-9 The ninth International Conference on Chemical & Process Engineering, 10-13 May 2009 - Rome, Italy.

Cullis, C.F. and Willatt, B.M., 1983, *Oxidation of methane over supported precious metal catalysts*. J. Catal., 83: 267-285.

Garetto, T.F., Apesteguia, C.R., 2000, *Oxidative catalytic removal of hydrocarbons over Pt/Al_2O_3 catalyst* - Catal. Today 62:189–199.

Hou, K. and Hughes, R., 2001, *The kinetics of methane steam reforming over a Ni/α-Al_2O_3catalyst*. Chem. Eng. Journal, Vol. 82, No. 1-3, 311-328.

Kolaczkowski, S.Y., Serbetcioglu S., 1996, *Development of combustion catalysts for monolith reactors: a consideration of transport limitations* - Appl. Catal. A Gen. 138:199–214.

Lee, J.H., Trimm, D.L. (1995): *Catalytic combustion of methane.* Fuel Processing Technology 42: 339-359

Niwa, M., Awano, K., Murakami, Y., 1983, *Activity of supported platinum catalysts for methane oxidation* - Appl. Catal. 7 (3): 317–325.

Otto, K., 1989, *Methane oxidation over Pt on .gamma.-alumina: kinetics and structure sensitivity* - Langmuir, 5 (6):1364–1369.

Vaccaro S., Ciambelli P., 2008a, *Modeling of Surface-bed Reactor for Endothermic and Exothermic Reactions Coupling*. ch. 30 of "Recent Advances in Modelling and Simulation", G. Petrone and G. Cammarata ed.s, I-Tech Education and Publishing, Wien, Austria, 580-605.

Vaccaro S., Ciambelli P., 2008b, *Modelling of a Catalytic Micro-Reactor for Process Intensification.* 7th International Workshop on Catalytic Combustion IWCC7 September 29 – October 1, 2008 at Lake Zurich, Switzerland..

Xu, J. & Froment, G.F., 1989, *Methane steam reforming, methanation and water-gas shift. I. Intrinsic kinetics*. A.I.Ch.E. Journal, Vol. 35, No. 1, 88-96.

Zanfir, M. and Gavriilidis, A., 2003, *Catalytic Combustion Assisted Methane Steam Reforming*. Chem. Eng. Sci., Vol. 58, No 17, 3947– 3960.